

A Comparison of the ITS-90 Among NPL, NIM, and CEM, Above the Silver Point Using High-Temperature Fixed Points

G. Machin · W. Dong · M. J. Martín · D. Lowe ·
Z. Yuan · T. Wang · X. Lu

Received: 4 March 2010 / Accepted: 6 July 2010 / Published online: 22 July 2010
© Her Majesty the Queen in Rights of the United Kingdom 2010

Abstract A prototype comparison of the ITS-90, as realized by NPL, NIM, and CEM, using high-temperature fixed points (HTFPs) of Co-C (1324 °C), Pt-C (1738 °C), and Re-C (2474 °C), is reported. The local realizations of ITS-90 temperatures were assigned by NPL, NIM, and CEM to their own set of HTFPs. NIM and CEM then transported their cells to NPL, and the ITS-90 temperatures of all three sets of cells were measured using a linear pyrometer. From these measurements, a comparison reference value (CRV) was derived. At the Co-C and Pt-C points, the deviation from the CRV was <0.1 °C for all three institutes; at the Re-C point, the deviation was <0.4 °C. These deviations are significantly less than the scale realization uncertainties ascribed by the individual institutes indicating that these uncertainty estimates are conservative and could be revised to smaller values. In addition, thermodynamic temperatures were determined for these HTFPs using the current value of the thermodynamic temperature for the copper point, namely, 1357.82 K. Given the consistent performance of the HTFPs, they should be seriously considered as scale comparison artifacts of choice when comparing primary realizations of the ITS-90 and of the thermodynamic temperature.

G. Machin (✉) · D. Lowe
Engineering Measurement Division, National Physical Laboratory (NPL), Teddington,
Middlesex, UK
e-mail: graham.machin@npl.co.uk

W. Dong · Z. Yuan · T. Wang · X. Lu
Heat Division, National Institute of Metrology (NIM), Bei San Huan Dong Lu No. 18,
Beijing 100013, China

M. J. Martín
Centro Español de Metrología (CEM), C/del Alfar, 2, 28760 Tres Cantos, Madrid, Spain

Keywords Comparison · Comparison reference value · Eutectics · High-temperature fixed points

1 Introduction

The ITS-90 above the silver point is realized using Planck's law in ratio form referenced to a blackbody cavity at the freezing point of one of the defining fixed points. Due to the relative looseness of the definition, there is some freedom in how to realize the scale; for instance, the reference fixed-point blackbody could be Ag, Au, or Cu, and the selection of wavelength, optical system, or detector of the pyrometer is left to the user's discretion [1].

Due to this variation, it is essential that regular comparisons of internationally realized and disseminated versions of the ITS-90 above the silver point are performed to ensure that the radiance temperature scales realized in different national measurement institutes (NMIs) are equivalent. Unfortunately, due to the lack of suitable (reference) artifacts, comparisons are not able to probe the equivalence of local realizations of the ITS-90 to the uncertainty levels claimed by NMIs as, for example, in CCT Key Comparison (KC) 5 which used tungsten strip lamps as the transfer artifacts [2]. However, the advent of high-temperature fixed points (HTFPs) [3] has resulted in artifacts that could be used in a KC to demonstrate the equivalence of locally realized NMI scales at high temperatures. Such artifacts have been used already to perform limited comparisons [4, 5].

This study reports the results of a prototype ITS-90 comparison undertaken between UK, Chinese, and Spanish NMIs. The comparison was performed by using HTFPs of Co-C, Pt-C, and Re-C belonging to each of the institutes. Each of these cells was assigned an ITS-90 temperature by its respective institute. The HTFPs of NIM and CEM were then transported to NPL, and the ITS-90 temperatures for each were measured using a linear pyrometer. The temperature differences between the three institutes relative to a comparison reference value (CRV) were derived from measurements of the HTFPs, and an uncertainty analysis was performed for the comparison results. Finally, thermodynamic temperatures were derived for the HTFPs using the current thermodynamic value for the copper point [6].

The measurement procedure, results, and outline uncertainty analysis are presented in this article. It is clear that the performance of the cells, in terms of temperature stability and robustness, was far superior to any previously reported method of scale comparison at these temperatures. Indeed, HTFPs may be the only practical way of conducting a KC that genuinely probes the claimed uncertainties of local realizations of the ITS-90 above the silver point in a rigorous way.

2 Temperature Scales and HTFPs of NPL, NIM, and CEM

In this section, the realization of the ITS-90 by the respective institutes is described and the ascription of t_{90} to the respective cells detailed. All uncertainties, unless stated otherwise, are standard uncertainties ($k = 1$). Corrections were made for the mean

effective wavelength for the pyrometers used in each institute. The point of inflection of the melt was used to assign a temperature to each HTFP cell.

2.1 Temperature Scale of NPL

The temperature scale of NPL uses a copper fixed-point blackbody [7] as its foundation. A small target size, silicon photodiode-based pyrometer, the LP3 [8], was used to realize the ITS-90. The nominal center wavelength of the pyrometer was about 650 nm with a bandwidth of 14 nm. Scale realization uncertainties range from 0.09 °C at 1000 °C, 0.19 °C at 1700 °C, to 0.41 °C at 2500 °C. The furnace used to realize the HTFPs of NPL, and also those of NIM and CEM while at NPL, was a Chino IR-R80 [9]. The NPL cells were assigned ITS-90 temperatures during the measurements of the NIM and CEM cells at NPL. The uncertainties assigned to the NPL HTFP cells were 0.12 °C for the Co-C, 0.20 °C for the Pt-C, and 0.40 °C for the Re-C.

2.2 Temperature Scale of NIM

A silver fixed-point blackbody is utilized as the ITS-90 defining fixed point for the NIM scale [10]. For the measurements reported here, the primary standard pyrometer of NIM (NIM-PSP) [10] was used to realize the ITS-90 above the Ag point. The nominal center wavelength of the pyrometer was about 660 nm with a bandwidth of 11.2 nm. Scale realization uncertainties range from 0.02 °C at 962 °C, 0.11 °C at 1700 °C, to 0.24 °C at 2474 °C [10]. Corrections were made for the nonlinearity and size-of-source effect (SSE) of the NIM-PSP [11]. A three-zone furnace, with a sodium heat-pipe liner and two Chino IR80 furnaces [9] were used to realize the silver point and HTFPs, respectively. For each type of HTFP, two cells were prepared and t_{90} values assigned to each. The furnace effect was investigated by realizing each HTFP in the two different Chino furnaces. To mitigate for possible pyrometer drifts, the silver point was realized just before or after the HTFP measurements on the same day. The furnace step for the Chino furnace for each HTFP realization was set at ± 20 °C, and four cycles of melting and freezing were used for each cell. Due to lack of knowledge of the state of the prior heat treatment of the NIM HTFPs, the value of the first cycle was ignored and the average of the last three used to assign the ITS-90 of NIM to the HTFP. The standard deviation was taken to represent the short-term repeatability of the measured cell temperatures. The uncertainties in assignment of the temperatures to the NIM HTFP cells were 0.11 °C for the Co-C, 0.19 °C for the Pt-C, and 0.38 °C for the Re-C [12].

2.3 Temperature Scale of CEM

The temperature scale of CEM uses a copper fixed-point blackbody as a reference. A linear standard monochromatic thermometer IKE LP2 working with an interference filter of a center wavelength of nominally 653 nm and a bandwidth of 12 nm is used to realize the ITS-90 [8]. Corrections are made for the SSE of the LP2. Scale realization

uncertainties range from 0.10 °C at 962 °C to 0.42 °C at 2500 °C; specifically, for the Co-C: 0.15 °C, for the Pt-C: 0.25 °C, and for the Re-C: 0.5 °C.

The furnace used to realize the HTFPs at CEM is a CHINO IR-R80 [9]. Three melt-freeze cycles were made for each HTFP with different temperature steps (Δt): 10 °C, 20 °C, and 30 °C. The temperature assigned to the HTFP is the mean of the three inflection points obtained from the melting curves. The measurements were repeated twice for each HTFP and, in the case of Pt-C and Re-C cells, a different combination of neutral filters for the LP2 (with nominal transmission values of 0.1 and 0.01, respectively) was used. The stability of the CEM LP2 was confirmed by measuring the copper point at the beginning and at the end of the measurements of the HTFPs. The reference photocurrent was found to be repeatable to an equivalent of 0.01 °C at the Cu point.

3 Measurements at NPL of HTFP ITS-90 Temperatures

The HTFPs of NIM and CEM were transported to NPL. The HTFP cells from each institute had different provenances. The NIM Pt-C and Re-C cells were made in-house. The NIM Co-C was constructed at the National Measurement Institute of Japan (NMIJ), using NIM supplied Co. The CEM cells were supplied by Chino. The NPL Pt-C and Re-C cells were made in-house. The NPL Co-C was made at NMIJ, using NPL supplied Co. In general, each cell consisted of a graphite crucible, having a blackbody tube with a 3 mm aperture. Some technical details of the NPL, NIM, and CEM HTFP cells are given in Table 1.

All the cells were inspected and found to be intact before installation in the NPL Chino furnace. The only anomaly was that the CEM Pt-C cell was underfilled. This was

Table 1 Design and construction details of HTFPs of NPL, NIM, and CEM used in the comparison

Institute	HTFP	Crucible length (mm)	Blackbody tube length (mm)	Metal supplier, purity claimed	Included CC sheet or grafoil ^a
NPL	Co-C	45	32	0.99998	Sleeve
NIM	Co-C	45	32	0.99998	Sleeve
CEM	Co-C	45	32	0.99999	b
NPL	Pt-C	40	32	0.99999	Sleeve
NIM	Pt-C	43	32	0.99999	Hybrid+ Support
CEM	Pt-C	45	32	0.99999	b
NPL	Re-C	40	32	0.99999	Hybrid
NIM	Re-C	45	32	0.99999	CC sheet
CEM	Re-C	45	32	0.99999	b

^a The term “sleeve” means an additional thin sleeve of graphite is included in the crucible between the crucible wall and the ingot. The term “hybrid” means that there is at least one layer of grafoil between the sleeve and the crucible outer wall. The term “support” means that there is a physical support between the blackbody tube and the sleeve

^b Chino would not disclose the internal design of their cells

clearly apparent when the cell was put on a bench, as it had an asymmetric distribution of mass. All the other cells appeared completely filled.

The Chino furnace was baked at approximately 2000 °C under vacuum for about 1 h before the measurements with the Co-C and Pt-C cells were initiated. For the higher temperature Re-C cell, the furnace was baked at 2500 °C for 1 h with a He and Ar purge, and then at 2000 °C under vacuum for another 1 h before cell installation.

The cells were installed into the NPL Chino furnace so that the back wall of each cell was in the same position. The CEM Co-C cell was used as received, wrapped in grafelt. The other two Co-C and all three Re-C cells, prior to installation, were wrapped in three layers of pure grafoil™ (supplied by Japanese company Toyo Tanso¹). The Pt-C cell of NIM was used as received, i.e., wrapped in grafelt, whereas the NPL and CEM Pt-C cells were wrapped in three layers of grafoil.

The measurement sequence that was followed for the cells was: Co-C (NPL, NIM, CEM, NPL), Pt-C (NIM, NPL, CEM, NIM), and Re-C (NPL, CEM, NIM, NPL). The repeated cell measurements were made to check if there was any difference caused by removing and installing cells. These measured temperature differences were: at Co-C: 0.00 °C, at Pt-C: 0.01 °C, and at Re-C: +0.08 °C. The furnace window was removed during each measurement, and a flow of argon was maintained for the Co-C and Pt-C points and a mixture of Ar and He for the Re-C point. The melts were initiated by the following sequence. The furnace was ramped in a controlled way ($20\text{ }^{\circ}\text{C} \cdot \text{min}^{-1}$) to approximately 20 °C below the nominal melting point. When the furnace had stabilized, the furnace was then ramped at $20\text{ }^{\circ}\text{C} \cdot \text{min}^{-1}$ to 20 °C above the nominal melting temperature, held at this value until melting was complete, then ramped down at $20\text{ }^{\circ}\text{C} \cdot \text{min}^{-1}$ to 20 °C below the freeze. A minimum of four melt and freeze cycles was performed each day. Typically a melt freeze cycle took about 30 min.

The radiance measurements were performed using the NPL linear pyrometer, LP3. The stability of the LP3 was confirmed at the beginning and end of each measurement sequence through use of the NPL Cu-point blackbody. All the NPL measurements reported in this article were performed at nominally 650 nm, corrected for the mean effective wavelength. Typical melt profiles for the fixed points are shown in Fig. 1a (Co-C), b (Pt-C), and c (Re-C).

4 Measurement Results

Table 2 gives the ITS-90 values of the point of inflection measured at NPL for the individual cells along with the mean and standard deviations of the values. Table 3 gives the temperature assignment of local scales to the point of inflection of the HTFP cells at NPL, CEM, and NIM. The main contribution to the uncertainty in both cases is the scale realization (including a contribution from the SSE of the pyrometers used). All measurements are affected by the furnace conditions (the so-called “furnace effect”), and this has assumed type B contributions of 0.03 °C, 0.05 °C, and 0.1 °C at the Co-C, Pt-C, and Re-C points, respectively. Note this is likely to be a

¹ The grafoil used was 0.38 mm thick permafoil. The thermal conductivity is $200\text{ W} \cdot \text{m}^{-1} \cdot \text{K}^{-1}$ parallel to the surface and $5\text{ W} \cdot \text{m}^{-1} \cdot \text{K}^{-1}$ perpendicular to the surface. The nominal purity of this grafoil is 0.99999.

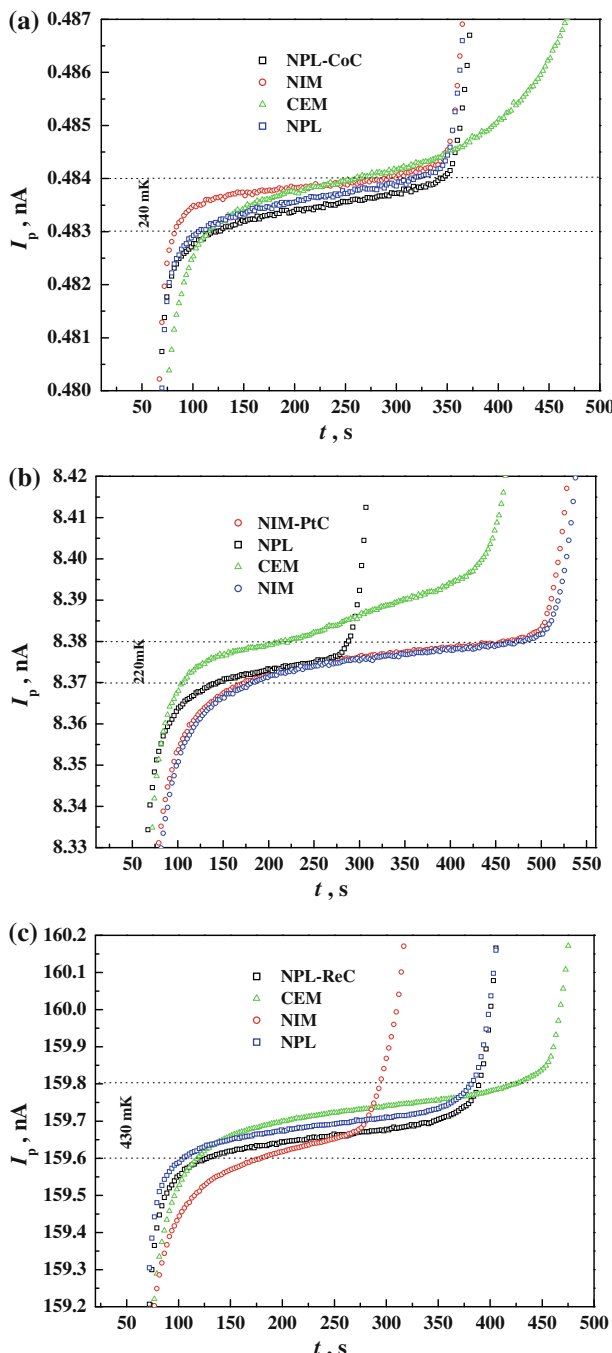


Fig. 1 Comparison of (a) Co-C, (b) Pt-C, and (c) Re-C melting curves of the NPL, NIM, and CEM cells. The CEM Pt-C cell clearly shows the effect of underfilling in premature breaking away from the melt curve

Table 2 ITS-90 temperatures of the HTFP cells of NPL, NIM, and CEM as measured at NPL

HTFP cell	Co-C (°C)	Pt-C (°C)	Re-C (°C)
NPL	1323.96	1737.86	2473.77
CEM	1323.99	1737.97	2473.83
NIM	1324.01	1737.88	2473.70
Average temperatures	1323.99	1737.90	2473.77
Standard deviation	0.03	0.06	0.07

The average temperatures of each type of cell and the standard deviation are also given

Table 3 ITS-90 temperatures of the HTFP cells of NPL, NIM, and CEM as measured at the respective institutes

HTFP cell	Co-C (°C)	Pt-C (°C)	Re-C (°C)
NPL	1323.96 (0.12)	1737.86 (0.20)	2473.77 (0.40)
CEM	1323.93 (0.15)	1737.97 (0.25)	2473.47 (0.50)
NIM	1324.01 (0.11)	1737.98 (0.19)	2474.14 (0.38)
CRV	1323.97	1737.94	2473.79
Standard deviation	0.04	0.07	0.34

These are known as the local temperatures. The average temperature of each type of fixed point is specified as the comparison reference value (CRV), and the standard deviation of this average is also given. The numbers in brackets are the uncertainties in temperature assignment by the individual institutes

very conservative estimate as an evaluation of the furnace effect by moving the Pt-C point 3 mm between realizations led to a measured temperature change of only approximately 0.02 °C. The following additional minor components were considered: drift of reference photocurrent during measurements (<0.01 °C) and the stability (or repeatability) of the point of inflection of each HTFP (<0.02 °C). These components are negligible in the uncertainty analysis. Both the aperture and length of the blackbody tube of all the HTFPs were the same and hence, the uncertainty due to variation in emissivity between cells was also very small.

4.1 Assessment of HTFP Quality

The individual HTFP melt profiles, as measured at NPL, are given in Fig. 1. From this, it can be observed that the Co-C and the Pt-C melting ranges are within 0.25 °C; for the Re-C, the range is a little larger at 0.4 °C. There are some interesting features to note. The Co-C cells for NIM and NPL are both the same design, though filled with different Co. The melting range and profile for these two cells is very similar. The CEM Co-C point left the melt less sharply than the other two Co-C points. This may have been due to the use of grafelt instead of grafoil for insulation around the cell. Nevertheless, the points of inflection for all three Co-C cells agree within 0.05 °C.

The Pt-C cells have different designs and quite different melt profiles. The NIM and NPL plateaux are quite different in duration, due to the NPL cell containing less material because it is shorter than the NIM cell. Despite this, the point of inflection

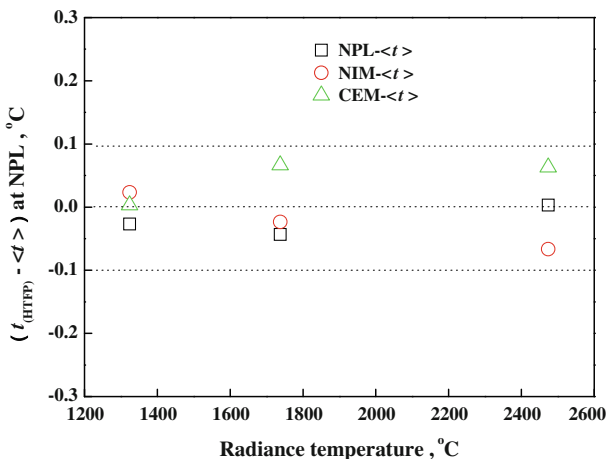


Fig. 2 Temperature differences of the individual HTFP cells from the mean ITS-90 value as measured at NPL

for the two melts differed by only 0.02 °C. The CEM cell is clearly continuing to melt for sometime after the point of inflection, evidenced by a kink in the melt profile. This is probably due to its being underfilled and not having a continuous solid/liquid interface enclosing the cavity. Despite this, its transition is at the highest temperature, indicating that very pure platinum was used. The points of inflection of the melts of the three Pt-C cells are in agreement to about 0.1 °C.

The Re-C cells are all well-filled and all display sharp exits from the melt. The NPL hybrid structure results in a longer melt than the NIM cell despite being a shorter cell with less fixed-point material. The NIM cell is slightly lower in temperature than the other two cells and has a slightly larger melting range indicating that the Re was not as pure as that used in the NPL and CEM cells. Despite this, the overall agreement of the three cells was about 0.1 °C.

The average temperatures of the HTFPs for all three institutes were determined (e.g., the averages of the NPL, NIM, and CEM Co-C points as measured at NPL), along with the standard deviations and are given in Table 2. This assessment was performed to determine how reproducible the point of inflection is for the individual cells for each material. Figure 2 shows the differences between the temperature of each HTFP and the mean temperature value for each type of HTFP. The NPL measured ITS-90 temperatures for each of the cells were in agreement to within 0.1 °C. These results confirm that HTFPs can now be made in a variety of designs, and manufactured by a number of different processes, but still show excellent reproducibility even for the highest temperatures.

4.2 Comparison of ITS-90 Realizations

The measurements of all the HTFP cells at NPL indicate that each type of cell *realizes the same temperature* to within 0.1 °C (Table 2). This allows a CRV to be calculated from the independent assignment of ITS-90 to each HTFP by each institute, with a

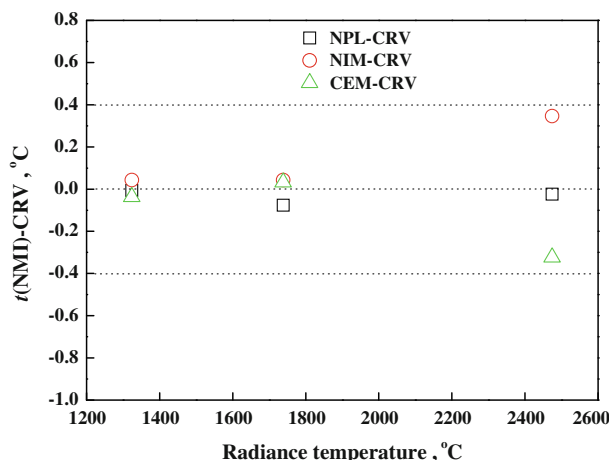


Fig. 3 Difference from the local realization of ITS-90 as realized by NPL, NIM, and CEM and the comparison reference value (CRV)

small allowance made in the uncertainty budget for the irreproducibility of the individual HTFPs. The simplest approach to calculate a CRV is to take the mean values of each local ITS-90 temperature assignment, i.e., the mean of the Co-C (or Pt-C or Re-C) ITS-90 temperatures as measured at NPL, NIM, and CEM. These assigned local ITS-90 temperatures, the means of these values, and the standard deviations are given in Table 3. The uncertainties in the temperature assignment are also given. One could introduce some sophistication in the determination of the CRV by weighting the individual values with the uncertainty of the evaluation, but for the purposes of this discussion, as the scale realization uncertainties in each institute are quite similar, it is not necessary. Figure 3 shows the temperature difference of each institute from the CRV value. All institutes are very close to the CRV at the Co-C and Pt-C points; there is a small deviation at the Re-C point but less than 0.4 °C. Pair-wise differences can be determined from Fig. 3 and degrees of equivalence calculated; this is the subject of another article [13].

4.3 Thermodynamic Temperatures for the HTFPs

CCT-WG4 has recently published a new best estimate for the thermodynamic temperature of the copper point, namely, 1357.82 K with a standard uncertainty of 0.02 °C ($k = 1$) [6]. This, along with the temperature measurement of the individual cells at NPL, can be used to estimate the thermodynamic temperatures of the Co-C, Pt-C, and Re-C points by using the new Cu-point value as the reference temperature. The estimated thermodynamic temperatures for these HTFPs, with standard uncertainties are: Co-C: (1324.06 ± 0.14) °C, Pt-C: (1738.02 ± 0.24) °C, and Re-C: (2473.98 ± 0.49) °C. These uncertainties include a type A component, namely that of estimating the average temperature value of the HTFP at NPL; the magnitude of this is taken to be the standard deviation in Table 2.

5 Discussion

The high-temperature scales of NPL, NIM and CEM are in very good agreement, with measured differences of $< 0.1^\circ\text{C}$ to the Pt-C point and $< 0.4^\circ\text{C}$ to the Re-C point, well within the standard uncertainty of scale realization for any one institute. It should be noted that CEM initially reported an ITS-90 value for their Re-C point of 2473.0°C , yielding quite a large deviation from the NPL and NIM values. After further investigation, it was found that the correction for the mean effective wavelength of the pyrometer had not been applied by CEM to the Re-C point ITS-90 temperature. This is a very good example of the diagnostic power of using stable and repeatable artifacts such as HTFPs in high-temperature measurement. In the past, such observed deviations might have been assigned to variation in the comparison artifact performance; however, this explanation was not plausible for these measurements, given the intrinsic stability of the HTFPs. These measurements allowed CEM to identify the omission and perform the correction.

As demonstrated, these artifacts are ideal for a comparison of independent local realizations of the ITS-90, or thermodynamic temperature. As such, any future KC of high-temperature scales should feature HTFPs. The excellent performance of the HTFPs means that a very stable KC reference value (KCRV) could be established even for very high temperatures, which has not been possible in the past due to the lack of suitable artifacts. Two points would need to be addressed: the comparison artifact temperatures should not be known, and the furnace conditions should be carefully controlled. The former is easily overcome by making the artifacts of slightly impure or deliberately doped material to adjust (slightly) their temperature away from the given value. The latter is a current subject of research, and either corrections or reasonable values for the uncertainty due to the furnace effect/conditions will be available in due course [14]. It should be noted that one benefit of having such repeatable high-temperature sources is that they could be used on a routine basis for confirming the realization of radiance scales to improve the robustness of the realization [15].

It is clear from the results obtained here that it is now possible to construct HTFPs (at least of Co-C, Pt-C, and Re-C) by different methods, with different designs, and different suppliers of materials and yet obtain very reproducible cells. This bodes well both for the primary temperature assignments to these HTFPs by the CCT-WG5 HTFP research plan in the next 2–3 years, and then for their establishment as reliable high-temperature references [14].

The values measured by NPL for all nine cells have been used to estimate the thermodynamic temperatures of the HTFPs. This was a straightforward calculation using the current value of the thermodynamic temperature for the copper point. As direct thermodynamic evaluations of the temperature of HTFPs become available through primary radiometry, it will be very interesting to compare those values with the ones obtained by reference to an ITS-90 defining fixed point (but substituting the thermodynamic value). These evaluations could help probe the thermodynamic fitness of ITS-90 above the silver point. In any event, it was very simple to derive thermodynamic values of these HTFPs from the Cu-point value, its thermodynamic uncertainty being so low (0.02°C) [6] as to make an insignificant addition to the uncertainty evaluation of the HTFPs by this method.

6 Conclusions

ITS-90 realizations above the silver point have been compared between three institutes: NPL, NIM, and CEM. Excellent agreement of the local scale realizations was found up to the Re-C point 2474 °C, well within the standard uncertainties of the scale realization for the individual institutes.

HTFPs are excellent artifacts for comparing high-temperature scales: either ITS-90 or thermodynamic temperature. These results strongly suggest that any future key comparison of high-temperature scales could be based on HTFPs.

Thermodynamic values of HTFPs can be simply estimated by the ratio method simply by substituting the thermodynamic value of the defining fixed point, rather than using its ITS-90 value, and by accounting for its assigned uncertainty.

Acknowledgment The NPL authors acknowledge funding from the National Measurement Office, an Executive Agency of the UK Department of Business, Innovation, and Skills.

References

1. H. Preston-Thomas, *Metrologia* **27**, 107 (1990)
2. CCT-K5, Realization of the ITS-90 between 961°C and 1700°C: 1997–1999, http://kcdb.bipm.org/appendixB/KCDB_ApB_info.asp?cmp_idy=457&cmp_cod=CCT-K5&prov=exalead. Accessed 04 Mar 2010
3. Y. Yamada, H. Sakate, F. Sakuma, A. Ono, *Metrologia* **38**, 213 (2001)
4. Y. Yamada, Y. Duan, M. Ballico, S.N. Park, F. Sakuma, A. Ono, *Metrologia* **38**, 203 (2001)
5. G. Machin, C.E. Gibson, D. Lowe, D.W. Allen, H.W. Yoon, in *Proceedings of TEMPMEKO 2004, 9th International Symposium on Temperature and Thermal Measurements in Industry and Science*, ed. by D. Zvizdić, L.G. Bermanec, T. Veliki, T. Stašić (FSB/LPM, Zagreb, Croatia, 2004), pp. 1057–1062
6. J. Fischer, M. de Podesta, K. Hill, M. Moldover, L. Pitre, P. Steur, O. Tamura, R. White, I. Yang, R. Rusby, M. Durieux, Document CCT/08-13rev, http://www.bipm.org/cc/CCT/Allowed/24/D13_rev_WG4_report_CCT_25_June_2008.pdf. Accessed 04 Mar 2010
7. B. Chu, H. McEvoy, J. Andrews, *Meas. Sci. Technol.* **5**, 12 (1994)
8. J. Hartmann, K. Anhalt, J. Hollandt, E. Schreiber, Y. Yamada, in *Proceedings of Temperatur 2003* (VDI-Bericht 1784, Berlin, 2003), pp. 135–141
9. Y. Yamada, N. Sasajima, H. Gomi, T. Sugai, in *Temperature: Its Measurement and Control in Science and Industry*, vol. 7, ed. by D. Ripple (AIP Conf. Proc., New York, 2002), pp. 985–996
10. Z. Yuan, X. Lu, C. Bai, J. Wang, W. Dong, X. Hao, T. Wang, submitted to *Int. J. Thermophys.*
11. W. Dong, Z. Yuan, P. Bloembergen, X. Lu, Y. Duan, submitted to *Int. J. Thermophys.*
12. Z. Yuan, T. Wang, X. Lu, W. Dong, C. Bai, X. Hao, Y. Duan, submitted to *Int. J. Thermophys.*
13. G. Machin, W. Dong, M.J. Martín, D. Lowe, Z. Yaun, T. Wang, X. Lu, *Metrologia* (in preparation)
14. G. Machin, P. Bloembergen, J. Hartmann, M. Sadli, Y. Yamada, *Int. J. Thermophys.* **28**, 1976 (2007)
15. G. Machin, *Acta Metrologica Sin.* **29**, 10 (2008)